

# Thermal dilepton polarization and dynamics of the QCD plasma in relativistic heavy-ion collisions

Xiang-Yu Wu,<sup>1</sup> Han Gao,<sup>1</sup> Bailey Forster,<sup>1</sup> Charles Gale,<sup>1</sup> Greg Jackson,<sup>2</sup> and Sangyong Jeon<sup>1</sup>

<sup>1</sup>*Department of Physics, McGill University, 3600 University Street, Montreal, QC H3A 2T8, Canada*

<sup>2</sup>*SUBATECH, Université de Nantes, IMT Atlantique, IN2P3/CNRS,  
4 rue Alfred Kastler, La Chantrerie BP 20722, 44307 Nantes, France*

(Dated: December 20, 2024)

We present the first theoretical study of the polarization of lepton pairs produced in  $\sqrt{s_{\text{NN}}} = 5.02$  TeV Pb+Pb collisions at the LHC, using next-to-leading order (NLO) dilepton emission rates. These calculations employ a multi-stage framework to simulate the evolution of relativistic heavy-ion collisions, and to explore the sensitivity of polarization to early times. It is found that the intermediate invariant-mass dileptons are indeed probes of the thermal equilibration process, and go beyond the reach of hadronic observables. We compute the polarization anisotropy coefficient obtained with LO dilepton rates, and show that the LO and NLO results differ radically, both in trend and in magnitude, at low and intermediate lepton pair invariant masses.

**Introduction.** — Relativistic heavy-ion collisions produce the quark-gluon plasma (QGP), an exotic state of matter described by quantum chromodynamics [1]. As the QGP expands and cools over the duration of a collision between two nuclei, the quarks can emit electromagnetic (EM) radiation which escapes the strongly interacting medium [2–7]. Therefore, photon and dilepton measurements have the potential to provide direct information about the hot medium, such as electric conductivity [8], chemical equilibrium [9–11], magnetic fields [12–15], and most notably, early-stage temperature [16–18]. Experimentally, EM probes have been recently measured in the Large Hadron Collider (LHC) [19] and the Relativistic Heavy-Ion Collider (RHIC) [20–22].

The  $p_{\text{T}}$ -spectrum of direct photons is sensitive to the local hydrodynamical flow, and can therefore inform the theoretical modeling [2]. In contrast, the invariant mass spectrum of dileptons — a complementary probe — is impervious to flow effects. For invariant mass  $M \gtrsim 1$  GeV, an important source of dileptons is quark-antiquark annihilation into a virtual photon (labeled from hereon LO, a leading-order contribution) [22–24] [25], yielding thermal, and also pre-equilibrium dileptons [9–11]. However, corrections from the strong interaction occur in the intermediate mass range (IMR),  $1 \text{ GeV} \lesssim M \lesssim 3 \text{ GeV}$ , and even become dominant in the low mass range (LMR):  $M \lesssim 1 \text{ GeV}$ . For completeness, one also defines a high mass range (HMR) as  $M \gtrsim 3 \text{ GeV}$ . We will focus on the thermal mechanism in what follows.

Because of the gluon’s abundance in a hot QGP medium, new channels open up at next-to-leading order (NLO) which includes: Compton scattering ( $gq \rightarrow \gamma^*q$  and  $g\bar{q} \rightarrow \gamma^*\bar{q}$ ), as well as modified annihilation ( $q\bar{q} \rightarrow \gamma^*g$  and  $q\bar{q}g \rightarrow \gamma^*$ , with the latter being kinematically suppressed for  $M \simeq 0$ ). Note that the above “real” gluon emissions need to be combined with the “virtual” (1-loop) corrections to  $q\bar{q} \rightarrow \gamma^*$  to obtain a finite result at strict NLO [26, 27]. As  $M \rightarrow 0$ , the strict expansion becomes invalid due to the physical necessity of thermal screening and the Landau-Pomeranchuk-Migdal (LPM)

effect. These are addressed in an effective theory (for small  $M$ ) which resums naively higher-order terms [28–31]. Both regimes can be systematically combined in the spectral function obtained in the thermal field theory, to cover both small and large  $M$  [32–34]. Together, the NLO and LPM contributions [35] are found to qualitatively enhance the observed thermal dilepton spectrum in the LMR, as well as in the IMR [17, 18, 36].

In addition to mass and  $p_{\text{T}}$  spectra, the polarization of EM radiation provides another unique tool to study medium properties. For example, the angular distribution of the thermal lepton pair in the rest frame of the virtual photon [37–39] [40] is expected to be sensitive to plasma anisotropy [41]; the same can be said for the polarization of real photons [42].

This work aims to provide a realistic study of the polarization of thermal dileptons produced in heavy-ion collisions at the LHC, using state-of-the-art multi-stage modeling calibrated to reproduce hadronic observables at  $\sqrt{s_{\text{NN}}} = 5.02$  TeV [9] together with strong coupling corrected EM production rates. We introduce the polarization coefficient, and highlight its explicit dependence on the local flow and the thermal spectral densities. We show how dilepton polarization in the IMR has the potential to reveal the importance of NLO contributions, and thus the role of gluons in the medium. We also show results for the LMR, with the understanding that processes involving composite hadrons will play a crucial role there [24], while being subdominant in the IMR. We also estimate polarization results for the elusive pre-equilibrium phase of relativistic heavy-ion collisions.

**Theoretical Setup.** — We consider a fluid cell in thermodynamic equilibrium, characterized by a four-velocity  $u^\mu$  and a temperature  $T$  [43]. The differential emission rate  $R_{\ell\bar{\ell}}$  of dileptons is [44]

$$E_+ E_- \frac{dR_{\ell\bar{\ell}}}{d^3\mathbf{p}_+ d^3\mathbf{p}_-} = -\frac{2e^4}{(2\pi)^6} \frac{\sum_i^{N_f} Q_i^2}{K^4} L^{\mu\nu} \rho_{\mu\nu} f_{\text{B}}(\omega). \quad (1)$$

Here,  $K = P_+ + P_-$  is the four-momentum of the virtual photon,  $f_{\text{B}}(\omega) \equiv \frac{1}{e^{\omega/T} - 1}$  is the Bose-Einstein distribu-

tion, and  $eQ_i$  is the charge of quark flavor  $i$ . In this work  $N_f = 3$ . The leptonic tensor is  $L^{\mu\nu} \equiv P_+^\mu P_-^\nu + P_-^\mu P_+^\nu - g^{\mu\nu}(P_+ \cdot P_- + m_\ell^2)$ , and the photon spectral function  $\rho_{\mu\nu}$  is a function of the two invariants  $\omega \equiv u \cdot K$  and  $k \equiv \sqrt{\omega^2 - K^2}$  (which correspond to the energy and momentum of the virtual photon in the medium's rest frame), formally obtained by analytic continuation of the Euclidean correlator  $G_{\mu\nu}$ :

$$\rho_{\mu\nu}(\omega, \mathbf{k}) \equiv -\text{Im} \left[ \int_0^{1/T} d\tau e^{i\omega_n \tau} G_{\mu\nu}(\tau, \mathbf{k}) \right]_{i\omega_n \rightarrow \omega + i0^+},$$

$$G_{\mu\nu}(\tau, \mathbf{k}) = \int d^3\mathbf{x} e^{-i\mathbf{k} \cdot \mathbf{x}} \langle J_\mu(\tau, \mathbf{x}) J_\nu(0, \mathbf{0}) \rangle_T, \quad (2)$$

where  $J_\mu = \bar{\psi} \gamma_\mu \psi$  is the EM current,  $\langle \dots \rangle_T$  denotes the thermal average, and  $\tau$  is the imaginary-time [45].

As the medium velocity  $u^\mu$  specifies a preferred direction, we can decompose  $\rho^{\mu\nu}$  into longitudinal and transverse parts, respectively as [46]

$$\rho_L \equiv -\frac{K^2 \rho_{\mu\nu} u^\mu u^\nu}{(u \cdot K)^2 - K^2}, \quad \rho_T \equiv \frac{\rho_\mu^\mu - \rho_L}{2}. \quad (3)$$

It is also useful to define the ‘‘vector channel’’ and the polarization difference, namely

$$\rho_V \equiv \rho_\mu^\mu = \rho_L + 2\rho_T, \quad \rho_\Delta \equiv \rho_T - \rho_L = \frac{\rho_V - 3\rho_L}{2}. \quad (4)$$

From Eq. (1), one can integrate the relative momentum of the  $\ell\bar{\ell}$ -pair to obtain the dilepton production rate in terms of the 4-momentum of the virtual photon alone,

$$\frac{dR_{\ell\bar{\ell}}}{d^4K} = \frac{2\alpha_{\text{em}}^2}{9\pi^2} \frac{\sum_i^{N_f} Q_i^2}{K^2} B\left(\frac{m_\ell^2}{K^2}\right) \rho_V f_B(\omega), \quad (5)$$

where  $B(\xi) \equiv (1 + 2\xi)\sqrt{1 - 4\xi}$  is a phase-space factor. As the equilibrium rate in Eq. (5) is proportional to  $\rho_V$ , observables such as dilepton invariant mass spectra and elliptic flow cannot differentiate between  $\rho_T$  and  $\rho_L$ .

Non-perturbative constraints on the spectral function can be obtained from lattice QCD simulations, where  $G_{\mu\nu}(\tau, \mathbf{k})$  is measured at fixed momenta  $k = 2\pi n/(aN_s)$  where  $n$  is an integer,  $a$  is the lattice spacing and  $N_s$  is the number of spatial sites. In practice, the analytic continuation to *real* frequencies is fraught with difficulty [47]. Yet significant progress has been made, first focusing on  $\rho_V$  [48]. However, the vector channel is insensitive to thermal physics owing to the large ultraviolet vacuum component of the photon self-energy. For this reason, it was suggested to consider the correlator  $\rho_\Delta$  which vanishes in vacuum and is highly suppressed for large  $\omega$  [49–51]. Recently, Ref. [52] of the HotQCD collaboration obtained estimates for  $\rho_\Delta(\omega, k)$  for 2+1 flavours [53] at  $T \simeq 220$  MeV with spatial momenta ranging from  $k \simeq 0.5$  to 1.4 GeV. Ubiquitously,  $\rho_\Delta$  decreases as a function of  $\omega$ , from positive at  $\omega = k$  and then quickly becoming negative for  $\omega > k$ . This is consistent with perturbation theory, where both  $\rho_T$  and  $\rho_L$  have been worked out at

strict NLO [26, 27], and also generalized to finite baryon density [18, 54].

Complementary to the lattice agenda,  $\rho_\Delta$  is also relevant for heavy-ion experiments, when it comes to the angular distribution of the final  $\ell\bar{\ell}$ -pair. The latter observable, in the rest frame of the virtual photon, discriminates between the longitudinal and transverse polarization. This angular distribution can be parametrized as

$$\frac{dN}{d^4K d\Omega_\ell} \propto 1 + \lambda_\theta \cos^2 \theta_\ell + \lambda_\phi \sin^2 \theta_\ell \cos 2\phi_\ell$$

$$+ \lambda_{\theta\phi} \sin 2\theta_\ell \cos \phi_\ell + \lambda_\phi^\perp \sin^2 \theta_\ell \sin 2\phi_\ell$$

$$+ \lambda_{\theta\phi}^\perp \sin 2\theta_\ell \sin \phi_\ell. \quad (6)$$

A common choice of the  $\gamma^*$  rest frame is the so-called helicity (HX) frame where the  $z$ -axis aligns with the momentum of the virtual photon [55]. Here, polar angles  $\Omega_\ell = (\theta_\ell, \phi_\ell)$  are defined in a way such that  $\ell^+$  in the HX frame has the 3-momentum  $\mathbf{l}_+ = l(\sin \theta_\ell \cos \phi_\ell, \sin \theta_\ell \sin \phi_\ell, \cos \theta_\ell)$ . By performing a change of variables and integrating out the radial part of dilepton relative momentum in Eq. (1), we arrive at an expression for the polarization coefficient  $\lambda_\theta$  of a single fluid cell at temperature  $T$ :

$$\lambda_\theta = \frac{3(\chi - \frac{1}{3})(1 - 4\xi)\rho_\Delta}{\frac{4}{3}(1 + 2\xi)\rho_V - (\chi - \frac{1}{3})(1 - 4\xi)\rho_\Delta}, \quad (7)$$

where  $\xi \equiv \frac{m_\ell^2}{K^2}$  and  $\chi \equiv \frac{(\mathbf{u}_* \cdot \hat{k})^2}{\mathbf{u}_*^2}$  with  $\mathbf{u}_*$  denoting the fluid velocity viewed in the HX frame. It is related to  $\mathbf{u}$  in the lab frame by a Lorentz boost

$$\mathbf{u}_* = \mathbf{u} + \left(\frac{\omega}{M} - 1\right) (\mathbf{u} \cdot \hat{k}) \hat{k} - \frac{u_0 \mathbf{k}}{M}. \quad (8)$$

One can work out the other coefficients from Eq. (6), in a similar manner. Nevertheless,  $\lambda_\theta$  is the only coefficient that does not vanish for a medium at rest, making it an indicator of  $\rho_\Delta$  that is less sensitive to local flow conditions. In this letter, we focus on  $\lambda_\theta$ .

We note that Eq. (7) is closely connected with  $\rho_\Delta$  [39]. Indeed, for a plasma at rest  $u^\mu = (1, \mathbf{0})$  (i.e.  $\chi = 1$ ), evaluating Eqs. (7) and (8) and assuming  $m_\ell \approx 0$  yields

$$\lambda_\theta = \frac{(1 - 4\xi)(\rho_T - \rho_L)}{\rho_L + (1 + 4\xi)\rho_T} \simeq \frac{\rho_\Delta}{\rho_T + \rho_L}, \quad (9)$$

which is displayed in Fig. 1.

Before embedding the fully differential rates on a hydrodynamical background, it is instructive to analyze Eq. (9) for small and large invariant masses, omitting flow conditions. Because the spectral functions are controlled by  $M/T$ , the large  $M$  limit can be viewed as  $T \rightarrow 0$  for a fixed  $M$ . The thermal medium becomes irrelevant from the perspective of a highly virtual photon. In this case,  $\gamma^*$  behaves as it was a massive vector field randomly produced in vacuum, having no preference in its orientation. Hence  $\lambda_\theta \rightarrow 0$  for both LO and NLO in the large  $M$

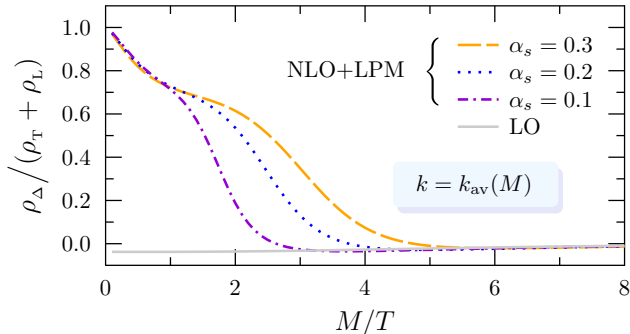


FIG. 1. Approximation to  $\lambda_{\theta}$  from the ratio of spectral functions in Eq. (9), as a function of the invariant mass  $M$  with  $k$  fixed by Eq. (10). The resummed NLO result is shown for fixed coupling,  $\alpha_s = \{0.1, 0.2, 0.3\}$ .

limit, as we shall see below. This asymptotic behaviour is indeed confirmed more quantitatively by the operator product expansion [56, 57], where it was found that  $\rho_{\Delta} \sim k^2(T/M)^4$  while  $\rho_{T,L} \sim M^2$  for  $M \gg T, k$ . For the opposite limit  $M/T \rightarrow 0$ , the virtual photon is more akin to a real photon, lacking the longitudinal polarization, so that  $\lambda_{\theta} \simeq (\rho_T - \rho_L)/(\rho_T + \rho_L) \rightarrow 1$ . This is indeed observed at NLO, as revealed by Fig. 1 where, for illustration, we evaluate the spectral functions at  $k = k_{av}(M)$  and  $\omega = \sqrt{M^2 + k^2}$ , with

$$k_{av}^2(M) \equiv \frac{\int_0^{\infty} dk k^4 \exp(-\frac{\sqrt{M^2+k^2}}{T})}{\int_0^{\infty} dk k^2 \exp(-\frac{\sqrt{M^2+k^2}}{T})} = \frac{3MT K_3(\frac{M}{T})}{K_2(\frac{M}{T})}, \quad (10)$$

$K_n$  being the modified Bessel function of the second kind. From Fig. 1, we note that the limit for  $M \ll T$  is robust even when varying  $\alpha_s$ . This physics is absent from LO calculations as the process  $q\bar{q} \rightarrow \gamma$  is kinematically forbidden, making the LO incapable of converging to the real-photon limit. Therefore the NLO correction is essential for studying polarization, especially in LMR, but also in the IMR. The rest of our study will use  $\alpha_s = 0.3$ , a value which is consistent with the bulk of phenomenological studies performed for collisions performed at the LHC [58].

**Thermal Dilepton Phenomenology.**— The relativistic event-by-event heavy-ion collisions of Pb+Pb at  $\sqrt{s_{NN}} = 5.02$  TeV are simulated using the iEBE-MUSIC framework [3, 59, 60], adopting the same model setup as in Ref. [9]. The production of lepton pairs is calculated as it was in Ref. [9]. The local temperature  $T(X)$ , and local flow velocity  $u^{\mu}(X)$  for each fluid cell at space-time point  $X = (t, \mathbf{x})$  are obtained to yield the polarization observables (at LHC energies, the baryon chemical potential  $\mu_B$  can be neglected). For a given lab-frame virtual photon four-momentum  $P$ , the final  $\lambda_{\theta}$  is a weighted average

over all fluid cells, namely

$$\lambda_{\theta}(P) = \frac{\int d^4X \lambda_{\theta}(P; T(X)) \mathcal{R}(P; T(X))}{\int d^4X \mathcal{R}(P; T(X))}, \quad (11)$$

where  $\mathcal{R}(P; T) \equiv \frac{dR_{\ell\bar{\ell}}}{d^4K}(K; T)/(1 + \lambda_{\theta}(P, T)/3)$  is the weight function obtained from integrating over  $d\Omega_{\ell}$  of the both sides of Eq. (6), and  $K^{\mu} = \Lambda_{\nu}^{\mu}(X)P^{\nu}$  is the virtual photon four-momentum in the local rest frame of the fluid cell at  $X$ , boosted according to the local  $u^{\mu}(X)$ . The invariant mass and transverse momentum, dependent  $\lambda_{\theta}(M)$  and  $\lambda_{\theta}(p_T)$ , are obtained in a similar way with complementary kinematics integrated out.

Figure 2 shows the anisotropy coefficient  $\lambda_{\theta}$  as a function of the invariant mass  $M$  in the 0-20% centrality class for Pb+Pb collisions at  $\sqrt{s_{NN}} = 5.02$  TeV. Notably, in the LMR the inclusion of NLO corrections changes the anisotropy coefficient qualitatively:  $\lambda_{\theta}(M)$  shifts from a near-zero negative to a sizeable positive value after considering the NLO correction (this feature is also evident in Fig. 1). Physically, this indicates that  $q\bar{q}$  annihilation tends to produce longitudinal polarization in the HX frame, while the gluon Compton scatterings are more likely to result in  $\gamma^*$  with transverse polarization.

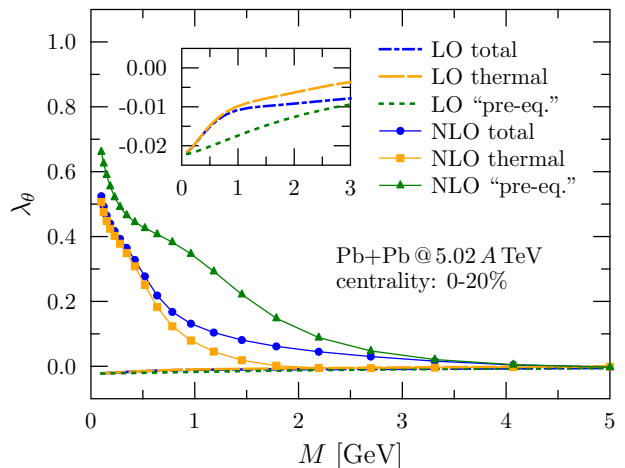


FIG. 2. The anisotropy coefficient  $\lambda_{\theta}$  of dilepton polarization with LO and NLO, induced by various sources, as a function of invariant mass  $M$  in the 0-20% centrality at  $\sqrt{s_{NN}} = 5.02$  TeV Pb+Pb collisions at the LHC. The inset figure shows the LO results scaled for clarity. Here, and in the rest of this letter, dilepton results are for dielectrons.

We note that  $\lambda_{\theta}$  given in Eq. (7), assuming  $m_{\ell} = 0$ , satisfies  $-\frac{1}{3} \leq \lambda_{\theta}|_{M \rightarrow 0} = \frac{1-3\chi}{\chi-3} \leq 1$ . The upper bound is saturated for  $\chi = 1$  (i.e.  $\mathbf{u}_* = 0$ ), as consistent with the behaviour of  $\rho_{\Delta}/(\rho_T + \rho_L)$  in Fig. 1. The lower bound occurs when  $\chi = 0$  (i.e.  $\mathbf{u}_* \cdot \hat{\mathbf{k}} = 0$ ), giving  $\lambda_{\theta} = \frac{-\rho_{\Delta}}{\rho_L + 3\rho_T} \rightarrow -\frac{1}{3}$  for  $M = 0$ . Therefore, once local flow conditions are included,  $\lambda_{\theta}$  at  $M \simeq 0$  limit will be slightly less than 1, as realized in Fig. 2 for the NLO re-

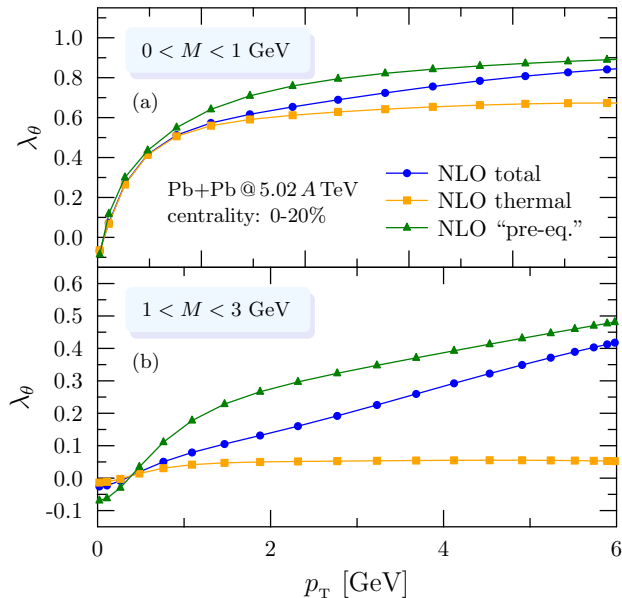


FIG. 3. The anisotropy coefficient  $\lambda_\theta$  of dilepton polarization evaluated at NLO, induced by various sources, as a function of transverse momentum  $p_T$  in the LMR (panel (a)) and IMR (panel (b)), for the 0-20% centrality class in Pb + Pb collisions at  $\sqrt{s_{NN}} = 5.02$  TeV.

sult. Nevertheless, although diluted by the plasma kinematics, the results obtained with NLO and LO rates are still radically different in the limit  $M \rightarrow 0$ , since the LO spectral function fails to capture the relevant physics in the IMR. In the HMR, QGP dileptons become almost unpolarized as  $\lambda_\theta \approx 0$ , consistent again with the pure thermal prediction in Fig. 2. However, the Drell-Yan process, the consideration of which lies beyond the scope of this study, is the main source of dilepton production and polarization in the HMR. In addition, Fig. 2 shows the effect on polarization of a pre-equilibrium contribution calculated with K $\phi$ MP $\phi$ ST as described in Ref. [2]. That pre-hydro addition, included in the “total” polarization, has a noticeable but relatively modest effect here.

In Fig. 3, we show  $\lambda_\theta$  as a function of transverse momentum  $p_T$  in the LMR and the IMR, where contributions from different stages of the fireball evolution are also displayed. In a given range of invariant mass,  $\lambda_\theta$  increases as a function of  $p_T$ . The behavior is consistent with that observed earlier: as the transverse momentum grows, the influence of the invariant mass shrinks, bringing the kinematics closer to those of real photons. In that limit, the transverse polarization dominates over the longitudinal. In the fluid dynamical environment, the exact value is also affected by the averaging over the flow. For the opposite limit  $p_T \rightarrow 0$ , we observe that  $\lambda_\theta$  does not vanish, which can also be attributed to the non-zero flow velocity of the medium in the HX frame of the dilepton.

Since gluon-mediated processes only contribute to dilepton polarization at NLO (and beyond), the corresponding enhancement of  $\lambda_\theta$  in the IMR window, if experimentally confirmed, could be taken as a flag for such elementary QCD interactions. Moreover, the behaviour of  $\lambda_\theta(p_T)$  could indicate the relative abundance of quarks and gluons: a larger  $\lambda_\theta(p_T)$  means a greater gluon-quark ratio during the pre-equilibrium stage than that in thermal equilibrium, as is clear in the bottom panel of Fig. 3. It is therefore very promising that the  $p_T$  dependence of  $\lambda_\theta$  in the IMR will offer valuable insights into the pre-equilibrium stage of heavy-ion collisions in future studies.

**Summary.**— In this letter, we perform the first study of dilepton polarization phenomenology using multi-stage heavy-ion collision simulations for  $\sqrt{s_{NN}} = 5.02$  TeV Pb+Pb collisions at the LHC. We employed NLO thermal emission rates in our analysis, which were coupled with the local temperature and flow velocity provided by the complete evolution history of the heavy-ion simulation.

We observe an overall sign change and a significant enhancement in  $\lambda_\theta$  when going from LO to NLO. This better matches the physical expectation that at small invariant mass, the virtual photon behaves like a real photon with *two* transverse polarization modes. In contrast, the LO calculation does not capture this aspect due to the vanishing phase space for  $M \rightarrow 0$ , where the NLO result is actually the “leading” contribution. At large invariant masses, the NLO result is a small correction to the LO one and both reflect the lack of a preferred polarization direction for  $M \gg T$ . Underlying this dramatic difference between orders in the perturbative calculation, is the participation of (thermal) gluons in the production reactions. The importance of gluons is readily supported from non-perturbative lattice studies, where the current-current correlators do not change qualitatively when going from quenched to 2+1 flavour QCD [49, 50, 52].

We also explore the dilepton polarization phenomenon induced during the pre-equilibrium stage and the QGP phase. It is found that dilepton polarization can be highly sensitive to the pre-equilibrium evolution; we find that the effects of the pre-equilibrium phase on dilepton polarization become more pronounced when considering the transverse momentum  $p_T$ -dependence in the IMR. Therefore, studies of the pre-equilibrium stages in heavy-ion collisions will benefit from those of dilepton polarization.

**Acknowledgements.**— This work was supported in part by the Natural Sciences and Engineering Research Council of Canada (NSERC) [SAPIN-2020-00048 and SAPIN-2024-00026], and in part by US National Science Foundation (NSF) under grant number OAC-2004571. G.J. was funded by the Agence Nationale de la Recherche (France), under grant ANR-22-CE31-0018 (AUTOTHERM). Computations were made on the Béluga super-computer system from McGill University, managed by Calcul Québec and by the Digital Research Alliance of Canada.



- [1] Barbara V. Jacak and Berndt Muller, “The exploration of hot nuclear matter,” *Science* **337**, 310–314 (2012).
- [2] Charles Gale, Jean-François Paquet, Björn Schenke, and Chun Shen, “Multimessenger heavy-ion collision physics,” *Phys. Rev. C* **105**, 014909 (2022), [arXiv:2106.11216 \[nucl-th\]](#).
- [3] Jean-François Paquet, Chun Shen, Gabriel S. Denicol, Matthew Luzum, Björn Schenke, Sangyong Jeon, and Charles Gale, “Production of photons in relativistic heavy-ion collisions,” *Phys. Rev.* **C93**, 044906 (2016), [arXiv:1509.06738 \[hep-ph\]](#).
- [4] Hendrik van Hees, Charles Gale, and Ralf Rapp, “Thermal Photons and Collective Flow at the Relativistic Heavy-Ion Collider,” *Phys. Rev. C* **84**, 054906 (2011), [arXiv:1108.2131 \[hep-ph\]](#).
- [5] Charles Gale and Kevin L. Haglin, “Electromagnetic radiation from relativistic nuclear collisions,” , 364–429 (2003), [arXiv:hep-ph/0306098](#).
- [6] Charles Gale and Joseph I. Kapusta, “Dilepton radiation from high temperature nuclear matter,” *Phys. Rev. C* **35**, 2107–2116 (1987).
- [7] Hendrik van Hees and Ralf Rapp, “Dilepton Radiation at the CERN Super Proton Synchrotron,” *Nucl. Phys. A* **806**, 339–387 (2008), [arXiv:0711.3444 \[hep-ph\]](#).
- [8] Ralf Rapp, “Electric Conductivity of QCD Matter and Dilepton Spectra in Heavy-Ion Collisions,” (2024), [arXiv:2406.14656 \[hep-ph\]](#).
- [9] Xiang-Yu Wu, Lipei Du, Charles Gale, and Sangyong Jeon, “Probing the equilibration of the QCD matter created in heavy-ion collisions with dileptons,” *Phys. Rev. C* **110**, 054904 (2024), [arXiv:2407.04156 \[nucl-th\]](#).
- [10] Oscar Garcia-Montero, Philip Plaschke, and Sören Schlichting, “Scaling of pre-equilibrium dilepton production in QCD Kinetic Theory,” (2024), [arXiv:2403.04846 \[hep-ph\]](#).
- [11] Maurice Coquet, Xiaojian Du, Jean-Yves Ollitrault, Soeren Schlichting, and Michael Winn, “Intermediate mass dileptons as pre-equilibrium probes in heavy ion collisions,” *Phys. Lett. B* **821**, 136626 (2021), [arXiv:2104.07622 \[nucl-th\]](#).
- [12] Xinyang Wang, Igor A. Shovkovy, Lang Yu, and Mei Huang, “Ellipticity of photon emission from strongly magnetized hot QCD plasma,” *Phys. Rev. D* **102**, 076010 (2020), [arXiv:2006.16254 \[hep-ph\]](#).
- [13] Xinyang Wang and Igor Shovkovy, “Photon polarization tensor in a magnetized plasma: Absorptive part,” *Phys. Rev. D* **104**, 056017 (2021), [arXiv:2103.01967 \[nucl-th\]](#).
- [14] Xinyang Wang and Igor A. Shovkovy, “Rate and ellipticity of dilepton production in a magnetized quark-gluon plasma,” *Phys. Rev. D* **106**, 036014 (2022), [arXiv:2205.00276 \[nucl-th\]](#).
- [15] Kento Kimura, Nicholas J. Benoit, Ken-Ichi Ishikawa, Chiho Nonaka, and Kenta Shigaki, “Estimate of virtual photon polarization due to the intense magnetic field in Pb-Pb collisions at the LHC energies,” (2024), [arXiv:2411.01406 \[hep-ph\]](#).
- [16] R. Arnaldi *et al.* (NA60), “NA60 results on thermal dimuons,” *Eur. Phys. J. C* **61**, 711–720 (2009), [arXiv:0812.3053 \[nucl-ex\]](#).
- [17] Jessica Churchill, Lipei Du, Charles Gale, Greg Jackson, and Sangyong Jeon, “Virtual Photons Shed Light on the Early Temperature of Dense QCD Matter,” *Phys. Rev. Lett.* **132**, 172301 (2024), [arXiv:2311.06951 \[nucl-th\]](#).
- [18] Jessica Churchill, Lipei Du, Charles Gale, Greg Jackson, and Sangyong Jeon, “Dilepton production at next-to-leading order and intermediate invariant-mass observables,” *Phys. Rev. C* **109**, 044915 (2024), [arXiv:2311.06675 \[nucl-th\]](#).
- [19] Shreyasi Acharya *et al.* (ALICE), “Dielectron production in central Pb–Pb collisions at  $\sqrt{s_{NN}} = 5.02$  TeV,” (2023), [arXiv:2308.16704 \[nucl-ex\]](#).
- [20] M. I. Abdulhamid *et al.* (STAR), “Measurements of dielectron production in Au+Au collisions at  $\sqrt{s_{NN}} = 27$ , 39, and 62.4 GeV from the STAR experiment,” *Phys. Rev. C* **107**, L061901 (2023).
- [21] L. Adamczyk *et al.* (STAR), “Measurements of Dielectron Production in Au+Au Collisions at  $\sqrt{s_{NN}} = 200$  GeV from the STAR Experiment,” *Phys. Rev. C* **92**, 024912 (2015), [arXiv:1504.01317 \[hep-ex\]](#).
- [22] “Temperature Measurement of Quark-Gluon Plasma at Different Stages,” (2024), [arXiv:2402.01998 \[nucl-ex\]](#).
- [23] R Arnaldi *et al.* (NA60), “Evidence for the production of thermal-like muon pairs with masses above 1 GeV/c<sup>2</sup> in 158 A GeV Indium-Indium Collisions,” *Eur. Phys. J. C* **59**, 607–623 (2009), [arXiv:0810.3204 \[nucl-ex\]](#).
- [24] Ralf Rapp, “Dilepton Spectroscopy of QCD Matter at Collider Energies,” *Adv. High Energy Phys.* **2013**, 148253 (2013), [arXiv:1304.2309 \[hep-ph\]](#).
- [25] This channel is also included in the Drell-Yan process where initial quarks are sourced from the nPDFs of the colliding ions.
- [26] M. Laine, “NLO thermal dilepton rate at non-zero momentum,” *JHEP* **11**, 120 (2013), [arXiv:1310.0164 \[hep-ph\]](#).
- [27] G. Jackson, “Two-loop thermal spectral functions with general kinematics,” *Phys. Rev. D* **100**, 116019 (2019), [arXiv:1910.07552 \[hep-ph\]](#).
- [28] Peter Brockway Arnold, Guy D. Moore, and Laurence G. Yaffe, “Photon emission from ultrarelativistic plasmas,” *JHEP* **11**, 057 (2001), [arXiv:hep-ph/0109064](#).
- [29] Peter Brockway Arnold, Guy D. Moore, and Laurence G. Yaffe, “Photon emission from quark gluon plasma: Complete leading order results,” *JHEP* **12**, 009 (2001), [arXiv:hep-ph/0111107 \[hep-ph\]](#).
- [30] P. Aurenche, F. Gelis, and H. Zaraket, “Enhanced thermal production of hard dileptons by  $3 \rightarrow 2$  processes,” *JHEP* **07**, 063 (2002), [arXiv:hep-ph/0204145](#).
- [31] P. Aurenche, F. Gelis, G. D. Moore, and H. Zaraket, “Landau-Pomeranchuk-Migdal resummation for dilepton production,” *JHEP* **12**, 006 (2002), [arXiv:hep-ph/0211036 \[hep-ph\]](#).
- [32] I. Ghisoiu and M. Laine, “Interpolation of hard and soft dilepton rates,” *JHEP* **10**, 083 (2014), [arXiv:1407.7955 \[hep-ph\]](#).
- [33] G. Jackson and M. Laine, “Testing thermal photon and dilepton rates,” *JHEP* **11**, 144 (2019), [arXiv:1910.09567 \[hep-ph\]](#).
- [34] J. Ghiglieri and M. Laine, “Smooth interpolation between thermal Born and LPM rates,” *JHEP* **01**, 173 (2022), [arXiv:2110.07149 \[hep-ph\]](#).
- [35] From this point on, we consider the “NLO contributions” to include the LPM resummation for small  $M$  as

- in Refs. [32, 33].
- [36] Jessica Churchill, Lipei Du, Bailey Forster, Han Gao, Greg Jackson, Sangyong Jeon, and Charles Gale, “Thermal dilepton production in heavy-ion collisions at beam-energy-scan (BES) energies,” *EPJ Web Conf.* **296**, 07006 (2024), arXiv:2312.10166 [nucl-th].
- [37] Enrico Speranza, Amaresh Jaiswal, and Bengt Friman, “Virtual photon polarization and dilepton anisotropy in relativistic nucleus–nucleus collisions,” *Phys. Lett. B* **782**, 395–400 (2018), arXiv:1802.02479 [hep-ph].
- [38] Minghua Wei and Li Yan, “Weak magnetic field effect on dilepton polarization in heavy-ion collisions,” *Phys. Rev. D* **110**, 054024 (2024), arXiv:2406.10041 [nucl-th].
- [39] Florian Seck, Bengt Friman, Tetyana Galatyuk, Hendrik van Hees, Enrico Speranza, Ralf Rapp, and Jochen Wambach, “Polarization of Thermal Dilepton Radiation,” (2023), arXiv:2309.03189 [nucl-th].
- [40] Also the centre-of-mass frame of the dilepton.
- [41] Maurice Coquet, Michael Winn, Xiaojian Du, Jean-Yves Ollitrault, and Soeren Schlichting, “Dilepton Polarization as a Signature of Plasma Anisotropy,” *Phys. Rev. Lett.* **132**, 232301 (2024), arXiv:2309.00555 [nucl-th].
- [42] Sigtryggur Hauksson and Charles Gale, “Polarized photons from the early stages of relativistic heavy-ion collisions,” *Phys. Rev. C* **109**, 034902 (2024), arXiv:2306.10307 [nucl-th].
- [43] The temperature is defined in the fluid rest frame.
- [44] Joseph I. Kapusta and Charles Gale, *Finite-Temperature Field Theory*, Cambridge Monographs on Mathematical Physics (Cambridge University Press, 2023).
- [45] Mikko Laine and Aleksi Vuorinen, *Basics of Thermal Field Theory*, Vol. 925 (Springer, 2016) arXiv:1701.01554 [hep-ph].
- [46] H. Arthur Weldon, “Covariant Calculations at Finite Temperature: The Relativistic Plasma,” *Phys. Rev. D* **26**, 1394 (1982).
- [47] Harvey B. Meyer, “Transport Properties of the Quark-Gluon Plasma: A Lattice QCD Perspective,” *Eur. Phys. J. A* **47**, 86 (2011), arXiv:1104.3708 [hep-lat].
- [48] J. Ghiglieri, O. Kaczmarek, M. Laine, and F. Meyer, “Lattice constraints on the thermal photon rate,” *Phys. Rev. D* **94**, 016005 (2016), arXiv:1604.07544 [hep-lat].
- [49] Bastian B. Brandt, Anthony Francis, Tim Harris, Harvey B. Meyer, and Aman Steinberg, “An estimate for the thermal photon rate from lattice QCD,” *EPJ Web Conf.* **175**, 07044 (2018), arXiv:1710.07050 [hep-lat].
- [50] Marco Cè, Tim Harris, Ardit Krasniqi, Harvey B. Meyer, and Csaba Török, “Photon emissivity of the quark-gluon plasma: A lattice QCD analysis of the transverse channel,” *Phys. Rev. D* **106**, 054501 (2022), arXiv:2205.02821 [hep-lat].
- [51] Harvey B. Meyer, Marco Cè, Tim Harris, Ardit Krasniqi, and Csaba Török, “Photon and dilepton production rate in the quark-gluon plasma from lattice QCD,” *PoS LATTICE2022*, 186 (2023).
- [52] Sajid Ali, Dibyendu Bala, Anthony Francis, Greg Jackson, Olaf Kaczmarek, Jonas Turnwald, Tristan Ueding, and Nicolas Wink (HotQCD), “Lattice QCD estimates of thermal photon production from the QGP,” *Phys. Rev. D* **110**, 054518 (2024), arXiv:2403.11647 [hep-lat].
- [53] Although these results were at a pion mass  $m_\pi \simeq 320$  MeV and not continuum extrapolated, the lattice was quite large with  $N_s = 96$  and  $a \simeq 7$  GeV<sup>-1</sup>.
- [54] Greg Jackson, “Shedding light on thermal photon and dilepton production,” *EPJ Web Conf.* **274**, 05014 (2022), arXiv:2211.09575 [hep-ph].
- [55] Pietro Faccioli, Carlos Lourenco, Joao Seixas, and Hermine K. Wohri, “Towards the experimental clarification of quarkonium polarization,” *Eur. Phys. J. C* **69**, 657–673 (2010), arXiv:1006.2738 [hep-ph].
- [56] S. Caron-Huot, “Asymptotics of thermal spectral functions,” *Phys. Rev. D* **79**, 125009 (2009), arXiv:0903.3958 [hep-ph].
- [57] M. Laine, M. Vepsalainen, and A. Vuorinen, “Ultra-violet asymptotics of scalar and pseudoscalar correlators in hot Yang-Mills theory,” *JHEP* **10**, 010 (2010), arXiv:1008.3263 [hep-ph].
- [58] M. Arslanok *et al.*, “Hot QCD White Paper,” (2023), arXiv:2303.17254 [nucl-ex].
- [59] Bjoern Schenke, Sangyong Jeon, and Charles Gale, “(3+1)D hydrodynamic simulation of relativistic heavy-ion collisions,” *Phys. Rev. C* **82**, 014903 (2010), arXiv:1004.1408 [hep-ph].
- [60] Björn Schenke, Sangyong Jeon, and Charles Gale, “Elliptic and triangular flow in event-by-event (3+1)D viscous hydrodynamics,” *Phys. Rev. Lett.* **106**, 042301 (2011), arXiv:1009.3244 [hep-ph].